Research paper

Computational performance comparison of multiple regression analysis, artificial neural network and machine learning models in turning of GFRP composites with brazed tungsten carbide tipped tool

A. Amith Gadagi[*] and B. Chandrashekar Adake

Department of Mechanical Engineering, KLE Dr. M. S. Sheshgiri College of Engineering & Technology, Belagavi, Karnataka, 590008, India

Abstract

In a turning process, it is essential to predict and choose appropriate process parameters to get a component's proper surface roughness (R_a). In this paper, the prediction of R_a through the artificial neural network (ANN), multiple regression analysis (MRA), and random forest method (machine learning) are made and compared. Using the process variables such as feed rate, spindle speed, and depth of cut, the turning process of glass fiber-reinforced plastic (GFRP) composite specimens is conducted on a conventional lathe with the help of a single-point HSS turning tool brazed with a carbide tip. The surface roughness of turned GFRP components is measured experimentally using the Talysurf method. By utilizing Taguchi's L27 array, the experiments are carried out and the experimental results are utilized in the development of MRA, ANN, and random forest method models for predicting the R_a. It is observed that the mean absolute error (MAE) of MRA, ANN and random forest for the training cases are found to be 39.33%, 0.56%, and 24.88%, respectively whereas for the test cases MAE is 54.34%, 2.59%, and 24.88% for MRA, ANN, and random forest, respectively.

1. Introduction

Glass fiber-reinforced plastic (GFRP) composite materials are widely used in the aircraft and automobile industries due to their excellent strength-to-weight ratio [1]. GFRP can be a substitute for conventional materials. Although these composites are mostly fabricated to a near shape, still some secondary machining operations like turning, milling, drilling, etc., are required. Rajasekaran *et al.* [2] conducted the

turning operation of the CFRP composite bars with the help of a ceramic cutting tool by taking into consideration the depth of cut and feed and cutting speed as turning process parameters. Experimentation was carried out based on Taguchi's orthogonal arrays, and further analysis of the variance was conducted to examine the effect of machining process variables on the surface finish of turned CFRP composites. Sarma *et al.* [3] in their work, used the design of experiments (DOE) for the conduction of the

machining experiments of GFRP composites and further optimized the cutting parameters for a better surface finish. They used a polycrystalline diamond tool in their work to machine the GFRP composites. Drilling process of GFRP composites was conducted to examine the impact of drilling parameters on machining performance indicators, namely thrust and surface finish. Experiments were performed in accordance with Taguchi's orthogonal arrays, and the machining parameters were optimized using grey relational analysis [4].

Prashanth *et al.* [5] conducted the milling studies on the GFRP by employing DOE and found that surface finish was affected by spindle speed, and feed rate is a key factor for the cutting force. In the end milling of GFRP, it was found that the life of tool was influenced by mainly the cutting speed then followed by feed rate and fiber orientation [6]. Ishwar *et al*. [7] employed an adaptive network Fuzzy inference system, popularly known as ANFIS, to develop the mathematical model relating surface roughness and material removal rate to a depth of cut, spindle speed, and feed rate in turning of stainless steel 202.

Experiments were performed using Taguchi's L16 array. The ANFIS and experimental results compared very well with each other. It was observed that the depth of cut has a major effect on Material Removal Rate (MRR), and surface finish was greatly affected by spindle speed. Manikandan *et al.* [8] utilized ANFIS for the prediction of surface finish, MRR, overcut, perpendicularity, and circularity error in wire electric discharge machining of metal matrix composites. The efficacy of ANFIS model in prediction was found to be high. The response surface methodology (RSM) technique was used to develop the empirical model to predict the machining performance characteristics like vibration, cutting temperature, and surface roughness. A CNC turning process was carried out on LM6/SiC$_p$ composites with the use of tungsten carbide inserts. The validation of empirical model was efficiently done through experimental results [9]. Grey regression analysis, which is based on Taguchi's technique, was utilized in optimizing machining process parameters in the milling operation of AISI 304 steel. The machining performance characteristics mainly chip reduction coefficient, surface roughness, and cutting forces were dealt

with their work for different cooling conditions like wet, cryogenic, and dry. It was found that cryogenic-cooled machining yielded better machining performance than dry and wet conditions [10].

Response surface methodology was used to obtain the optimal turning parameters for better surface finish as well as cutting forces of Al-6061-SiC-Gr nanocomposites. Experiments were conducted by taking the machining parameters, namely feed, cutting speed, and depth of cut. The tool wear was found to be negligible in the turning operation of nanocomposites. The results revealed the fact that cutting speed has a little influence on the cutting force. The predicted results were found to be in good agreement with those of experimental values [11]. A Non dominated sorting algorithm was utilized in optimizing the process parameters of the CNC milling operation of P20 mold steel, which involves deep cryogenic treatment (DCT). The process variables considered were feed rate, cutting speed, soaking duration, and depth of cut. The machining characteristics investigated were power consumption and cutting forces. It was observed that a DCT tool, which was soaked for a greater duration, minimizes power consumption and cutting forces [12]. In an end milling process of carbon fiber reinforced plastics (CFRP), optimizing the machining process variables, namely depth of cut, feed rate, and spindle speed was carried out using particle swarm optimization (PSO). Palanikumar *et al.* [13] employed a carbide tool (K10) to turn the GFRP components by considering fiber orientation, feed, cutting speed, machining time, and depth of cut. In their work, the optimal machining parameters were determined through Taguchi and Fuzzy logic approaches. Further, in year 2007, the multi-objective optimization of machining performance indicators of GFRP turned specimens, namely specific cutting pressure, material removal rate, tool wear, and surface roughness through Grey relational analysis [14].

Harish *et al.* [15] in their work employed artificial neural network (ANN) to estimate the chatter which occurs in turning operation. ANN was found to be efficient in the prediction of chatter with an accuracy of more than 90%. Goel *et al.* [16] performed a multi-response optimization of machining performance characteristics using

Grey regression analysis for better surface quality in the turning operation of a mono-crystalline germanium specimen. The turning process parameters dealt with were rake angle, depth of cut, feed rate, spindle speed, and tool overhang. The surface roughness, profile error, and waviness error were considered as the machining performance characteristics. Experiments were carried out as per the DOE. Francisco *et al.* [17] built the MRA prediction model for predicting the machining forces in the turning operation of carbon-reinforced PEEK CF30 specimens by taking depth of cut, cutting forces, and feed as the process parameters. Experiments were performed as per the full factorial design. The developed quadratic regression equation predicted the cutting forces with adequate accuracy. Sarma *et al.* [18] used the RSM technique to build the predictive model for cutting force as a function of machining process parameters in a turning operation of GFRP composite specimens using CBN tools. Mistry *et al.* [19] successfully employed random forest method in a new vehicle prediction technique for computational toxicology. In their work, they modeled the influences on the drug toxicity by different vehicles. Zhou *et al.* [20] utilized the concept of random forest for the prediction inflow prediction in wastewater treatment plants by considering the parameters like domestic water usage patterns and weather features. Zhang *et al.* [21] successfully modeled a robotic grasp detection using the random forest method with the help of an image processing technique. Kwak *et al.* [22] predicted the mechanical properties of γ-TiAl alloys, such as interlamellar space, nanoindentation hardness, elongation, and tensile strength with the use of the random forest method. Wang *et al.* [23] predicted solubility of carbon dioxide in the deep eutectic solvents with the use of the random forest method by considering variables such as hydrogen bond donors, molar ratio, hydrogen bond acceptors, pressure range, and temperature range. Li *et al.* [24] predicted whether the patients were at risk for contrast-induced nephropathy following coronary angiography. A detailed literature survey reveals the fact that there are no such works, which compare the prediction accuracy of the techniques, namely MRA, ANN, and machine learning algorithms. From the literature review, it can also be found

that the surface roughness of the turned GFRP composites using the brazed tungsten carbide tipped cutting tool has never been investigated. Therefore, this aspect is considered in the current work, where the turning operation of GFRP composites is carried out with a carbide-tipped cutting tool. The prediction models are developed through the previously discussed techniques and a comparative study pertaining to their prediction accuracy is dealt with.

2. Experimental method

The turning of GFRP composite specimens is carried out on a conventional lathe (Kirloskar Enterprise 1330), whose specifications are as given in Table 1. Turning process was used by a brazed carbide tipped single-point cutting tool. The composite specimen used in this work is shown in Fig. 1, and the mechanical properties, as per the manufacturer's specification, are given in Table 2. The GFRP composite bars used are of length of 125 mm and a diameter of 50 mm. Experiments are conducted by taking the turning parameters, namely feed rate, spindle speed, and depth of cut. A 3-level design was chosen for the process variables. The details of the levels chosen are as given in Table 3.

Table 1. Technical specifications of kirloskar enterprise 1330 lathe machine.

Parameter	Value
Motor power (kW)	2.25
Spindle speed (rpm)	54-1200
Compound slide travel (mm)	100
Cross slide travel (mm)	210
Longitudinal feed (mm/rev)	0.045-0.676
Spindle bore (mm)	41
Center height (mm)	175
Machine base (mm)	610
Machine height (mm)	750

Fig. 1. GFRP composite specimen.

Based on the 3-input levels and 3-input factors, Taguchi's L27 array is chosen and given in Table 4. The experiments are carried out as per DOE. Surface roughness of the turned composite specimens is measured by Taylor Hobson Form Talysurf surface roughness tester (Table 5).

Table 2. Mechanical properties of glass epoxy laminated fiber reinforced plastic.

Sl.no	Parameter	Value
1	Specific gravity (g/cm^3)	1.95
2	Tensile strength (N/mm^2)	250
3	Compressive strength (N/mm^2)	400
4	Flexural Strength (at room temperature) (N/mm^2)	350
5	Shear strength (N/mm^2)	120
6	Charpy impact (Kj/mm^2)	75

Table 3. Levels of input for DOE.

Level	Feed rate (mm/rev)	Spindle Speed (rpm)	Depth of cut (mm)
1	0.051	90	0.2
2	0.059	315	0.4
3	0.065	500	0.6

Table 4. Taguchi's l27 orthogonal array.

SL No	Feed rate (mm/rev)	Depth of cut (mm)	Spindle speed (rpm)	R$_a$ (μm)
1	0.051	0.2	90	2.99
2	0.051	0.2	315	4.4
3	0.051	0.2	500	2.28
4	0.051	0.4	90	4.82
5	0.051	0.4	315	5.12
6	0.051	0.4	500	2.7
7	0.051	0.6	90	4.36
8	0.051	0.6	315	3.24
9	0.051	0.6	500	3.5
10	0.059	0.2	90	3.1
11	0.059	0.2	315	3.68
12	0.059	0.2	500	2.98
13	0.059	0.4	90	2.49
14	0.059	0.4	315	2.91
15	0.059	0.4	500	2.91
16	0.059	0.6	90	4.05
17	0.059	0.6	315	0.88
18	0.059	0.6	500	2.65
19	0.065	0.2	90	3.98
20	0.065	0.2	315	1.94
21	0.065	0.2	500	3.6
22	0.065	0.4	90	3.6
23	0.065	0.4	315	3.33
24	0.065	0.4	500	2.97
25	0.065	0.6	90	4
26	0.065	0.6	315	5.85
27	0.065	0.6	500	0.51

Table 5. Technical specifications of Taylor Hobson form Talysurf surface roughness tester.

Parameter	Value
Traverse length (max/min)	200 mm/100 mm
Measuring speed range (mm/s)	0.1 to 1
Traverse speed (max, mm/s)	10
Data sampling interval (μm)	0.125 to 1
Resolution (nm)	0.6
Range to resolution ratio	1562500:1
Weight of traverse unit (kg)	15

3. Multiple regression analysis

Multiple regression analysis is a statistical technique through which the relation between the dependent and independent process variables is established. In the present work, the MRA technique is used to formulate the mathematical model for the surface roughness in terms of machining parameters, namely feed rate (F), depth of cut (Doc), and spindle speed (N). Multiple regression analysis is performed in MINITAB 17 statistical software. The developed mathematical model is as per Eq. (1):

$$y = \beta_0 + \beta_1 x_1 + \cdots + \beta_n x_n + \varepsilon \qquad (1)$$

y = output variable, x = input variable, ε = error

By utilizing the experimental data from Table 3 a multiple regression equation is formulated in MINITAB 17 software is represented by Eq. (2):

$$MRR = 45.4 - 1524 * F + 10.1 * Doc + 0.008 * N - 54 * F * Doc - 0.034 * F * N - 0.00921 * Doc * N + 13161 * F^2 - 5.2 * N^2 - 0.000008 * Doc^2 \qquad (2)$$

where N is the spindle speed (rpm), F is the feed rate (mm/rev), and Doc is the depth of cut (mm). The predictions of R$_a$ done, as per Eq. (2), are compared with the corresponding experimental values for the conformal test cases and the data sets used to build the MRA equation. A comparative graph of MRA predicted values vs. experimental values for the data sets used in building the MRA equation and test data is given in Fig. 2 and Fig. 3, respectively. The prediction error for each test case is tabulated in Table 6.
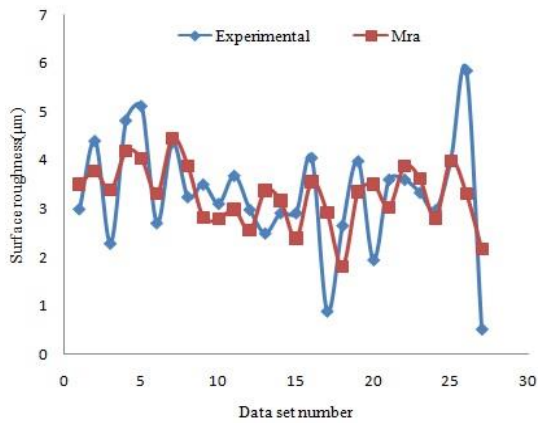
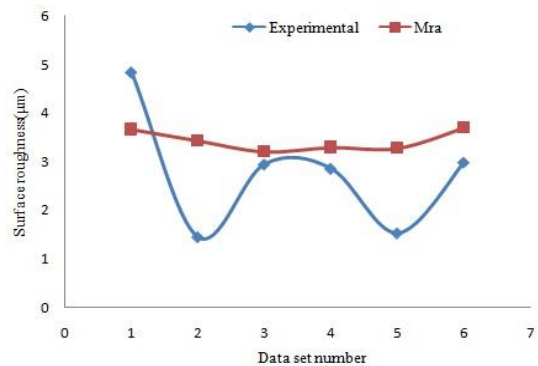**Fig. 2.** Comparison of surface roughness of L27 data sets vs. experimental values.

Fig. 3. Comparison of surface roughness of test cases of MRA vs. experimental values.

Table 6. Comparison of experimental surface roughness with MRA predicted surface roughness.

Feed rate (mm/rev)	Depth of cut (mm)	Spindle speed (rpm)	Expt. R_a (μm)	MRA R_a (μm)	Error (%)
0.053	0.4	315	4.84	3.65	24.40
0.057	0.5	224	1.44	3.42	138
0.058	0.3	140	2.94	3.20	8.98
0.061	0.3	224	2.85	3.28	15.4
0.062	0.4	315	1.52	3.27	115
0.063	0.5	140	2.98	3.69	23.8

4. Artificial neural network

ANN is analogous to a human brain, which has the capability to establish the non-linear and complex relationship between the dependent and independent variables. ANN can learn from the existing history and can perform the tasks of prediction and classification. An ANN structure basically has an input layer, an output layer, and hidden layers. The count of neurons in the input

and output layer is dependent on the number of input and output parameters, respectively. The neurons of an ANN structure are interconnected by synaptic connections, the strength of which depends on the values of the weights. A feed forward-back propagation ANN is selected in the present work. The count of input neurons in the present ANN structure is 3 which corresponds to the input process variables feed rate, depth of cut, and spindle speed, respectively, and the details of the network are shown in Fig. 4. A single neuron in the output layer represents the surface roughness of the turned GFRP specimens.

A MATLAB neural network toolbox is used to build the ANN model. Numerous ANN architectures were tried for the evaluation of surface roughness by considering different activation functions for the neurons. But the 3-20-20-1 ANN architecture resulted in a minimum mean square error (MSE) amongst all other architectures that were tried. Thus a 3-20-20-1 ANN structure, which is shown in Fig. 5, is selected based on the performance trials, for which the MSE is minimum and has a value of 0.00098379. The activation function for both the hidden layers is selected as 'TANSIG', and for the output layer a PURELIN function is chosen. The mathematical representation of PURELIN and TANSIG activation functions are given by Eqs. (3 and 4), respectively.

$$y = cx \qquad (3)$$

$$y = \frac{e^x - e^{-x}}{e^x + e^{-x}} \qquad (4)$$

where 'y' is the output response of the neuron, and 'x' is the total input to the neuron.
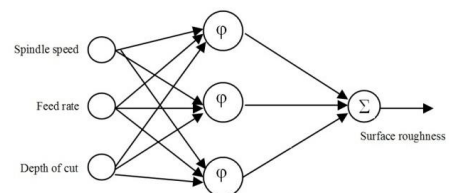

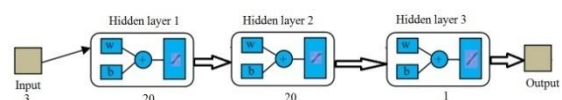**Fig. 4.** A general ANN structure [25].

Fig. 5. A 3-20-20-1 ANN structure used in MATLAB.

The training and learning algorithms chosen are 'TRAINLM' and 'LEARNGDM', respectively. A plot of MSE, training state, and regression coefficient are given in Figs. 6-8, respectively. The comparison plot of surface roughness for the training data set versus experimental, and testing data set versus experimental are shown in Fig. 9 and Fig. 10, respectively.
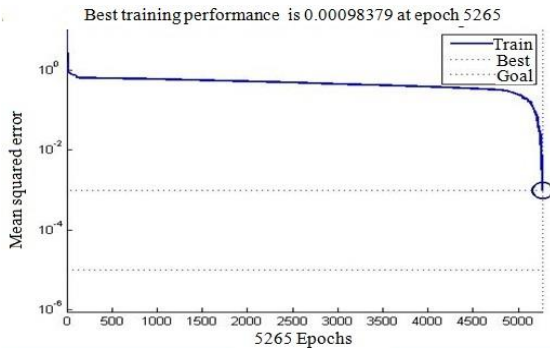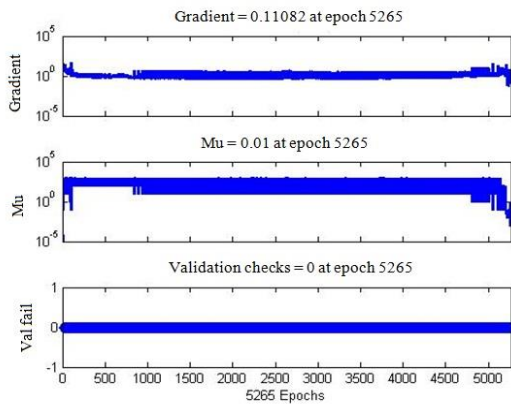

Fig. 6. Mean squared error.

Fig. 7. Training state of a 3-20-20-1 ANN structure.
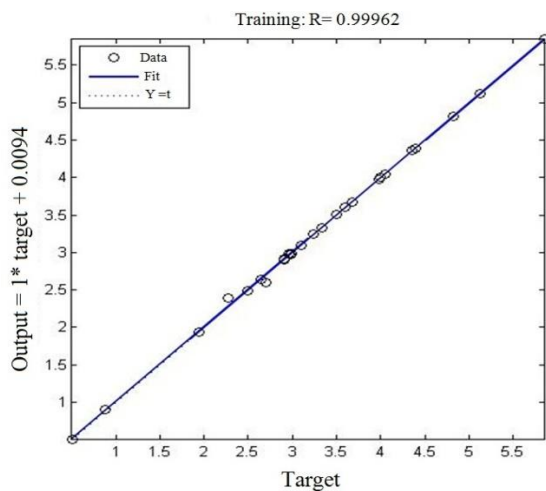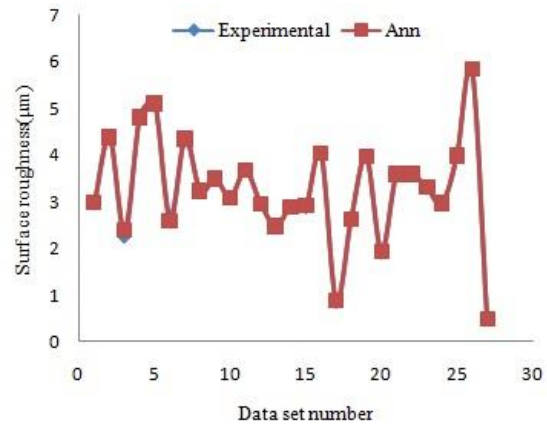

Fig. 8. Regression plot.

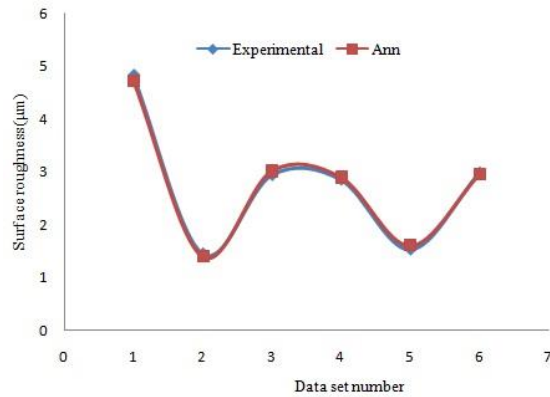**Fig. 9.** Comparison of surface roughness of ANN training data vs. experimental values.

Fig. 10. Comparison of surface roughness of ANN test data vs. experimental values.

5. Random forest method (machine learning algorithm)

The random forest method is basically a machine learning technique, which relies mainly on statistical models. It is basically an ensemble learning technique in which multiple classifiers are integrated to solve a complex problem. It generates decision trees that are based on random selection of the data sets and makes the prediction from each tree and obtains the best solution with the help of voting. It is a supervised learning method, which can be used for regression and classification purposes. It comprises many decision-making trees, and the robustness of the algorithm depends on the number of trees used. The random forest tree consists of 3 main components, namely the decision node, root node, and leaf node. The root

node gets split into the decision nodes and nodes whose further splitting is not possible are called leaf nodes. Followings are the steps involved in the building of the random forest model:

1. From the set of M observations and N features of the training data set, the samples are taken randomly.
2. A subset of N features is taken randomly and the feature which yields the best split is utilized to split the nodes in an iterative manner.
3. Growth of a tree is done to the largest extent by splitting the nodes. A node having the lowest impurity is selected for splitting. The impurity for a node is calculated by the Gini index, which is expressed by Eq. (5).

$$\text{Gini index} = 1 - \sum_{j=1}^{j=m}(P_j)^2 \qquad (5)$$

where, m = node and P_j = Probability of each class.
4. Steps 1-3 are repeated, and the prediction is obtained on the basis of the average prediction of all the trees as expressed by Eq. (6).

$$\bar{\varphi} = \frac{1}{T}\sum_{t=1}^{t=T}\varphi_t\,(q') \qquad (6)$$

where q' = samples, T = number of trees, φ_t = prediction of each tree, $\bar{\varphi}$ = average prediction of all the trees.
Random forest method is employed in the present work to estimate the R_a values for the independent variables feed rate, spindle speed, and depth of cut. Followings are the details of the random forest parameters used in this study:

n_estimators: 1000
max_depth: None
max_features: 'auto'
bootstrap: True
criterion: 'mse'
max_leaf_nodes: None
min_impurity_decrease: 0.0
min_impurity_split: None
min_samples_leaf: 1
min_samples_split: 2
min_weight_fraction_leaf: 0.0
n_jobs: None
oob_score: False
random_state: None

verbose: 0
warm_start: False.

The predictions done for the training and test data sets using the random forest method are compared with the experimental values in Fig. 11 and Fig. 12, respectively.

6. Results and discussion

In the current investigation, the surface roughness is considered as a turning performance indicator, while spindle speed, depth of cut and feed rate are considered as the turning process variables. The experimental results are used to develop and validate the MRA, ANN and machine learning numerical models.
A total of 27 experimental readings are used to develop the numerical prediction models, and 6 experimental results are used for the validation of the predictive models.
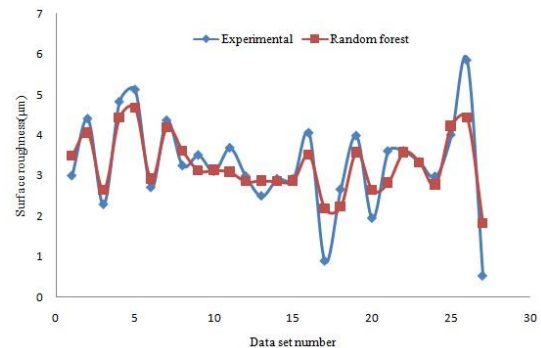

Fig. 11. Comparison of R_a of machine learning training data vs. experimental values.
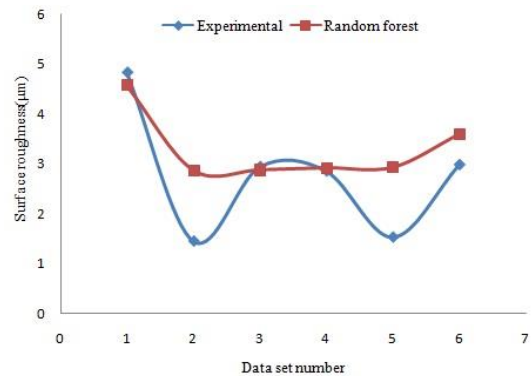

Fig. 12. Comparison of R_a of machine learning testing data vs. experimental values.

For the multiple regression analysis model, a quadratic function is employed to build the relationship between the independent and dependent variables. The MRA results predicted as per Eq. (2) are plotted for the L27 dataset and testing dataset in Fig. 2 and 3, respectively. The plot shows a large deviation between the predicted values of surface roughness and the corresponding experimental results. A 3-20-20-1 ANN structure is built using the MATLAB neural network toolbox, where the regression value is of the magnitude 0.99962 for training from Fig. 8. This value indicates that the efficacy of the ANN model is considerably higher. The ANN model used in the present study yielded a least MSE of 0.00098379 at an epoch of 5265, as shown in Fig. 6. Further, the gradient and learning rate at an epoch of 5265 are found to be 0.11082 and 0.01, respectively, which are shown in Fig. 7. From Fig. 9, it can be seen that the ANN predicted values for the training data set compares very well with that of the corresponding experimental values. From Table 5, it can be seen that the maximum error in the prediction is as low as 5%. From Fig. 10, it can be depicted that the ANN computed values for the testing data set are in good agreement with the experimental values. The MRA predicted values and the corresponding prediction errors with respect to experimental values for the test cases are listed in Table 6, while the details of the same for the ANN and machine learning models are given in Tables 7 and 8, respectively. It can be found from Tables 6-8 that, except for the first test case the prediction errors are considerably higher in the MRA model. The results, as predicted by a back propagation ANN structure, appears to be highly accurate as compared to the MRA and machine learning models. The reason for the large error associated with random forest could be attributed to the combined effect of a highly complex relationship between the dependent, independent variables in the data set, and lesser training instances.

From Table 9, which is a rank-defining table as calculated by MINITAB17, it is clear that the spindle speed has a greater effect and depth of cut has the least on the surface roughness while the feed rate has a moderate effect on the R_a.

Table 7. Comparison of experimental R_a with ANN predicted R_a.

Feed rate (mm/rev)	Depth of cut (mm)	Spindle speed (rpm)	Expt. R_a (μm)	ANN R_a (μm)	Error (%)
0.053	0.4	315	4.84	4.72	2.37
0.057	0.5	224	1.44	1.39	3.24
0.058	0.3	140	2.94	3.00	2.33
0.061	0.3	224	2.85	2.89	1.41
0.062	0.4	315	1.52	1.59	5.00
0.063	0.5	140	2.98	2.94	1.17

Table 8. Comparison of experimental R_a with machine learning predicted R_a.

Feed rate (mm/rev)	Depth of cut (mm)	Spindle speed (rpm)	Expt. R_a (μm)	Ml R_a (μm)	Error (%)
0.053	0.4	315	4.84	4.58	5.37
0.057	0.5	224	1.44	2.87	99.30
0.058	0.3	140	2.94	2.88	2.04
0.061	0.3	224	2.85	2.92	2.45
0.062	0.4	315	1.52	2.93	92.76
0.063	0.5	140	2.98	3.6	20.80

Table 9. Factor ranking based on mean effects.

Level	Feed rate (mm/rev)	Depth of cut (mm)	Spindle speed (rpm)
1	3.712	3.217	3.710
2	2.85	3.428	3.483
3	3.309	3.227	2.678
Delta	0.862	0.211	1.032
Rank	2	3	1

7. Conclusions

In the present work, the turning operation of GFRP specimens is performed on a conventional lathe using a brazed carbide tool by considering spindle speed, depth of cut, and feed rate as the process parameters. Experiments are conducted as per Taguchi's L27 orthogonal array, and the corresponding experimental values are used to develop multiple regression, artificial neural network, and machine learning prediction models. Followings are the conclusions of this work:

1. The maximum prediction error for multiple regression, ANN, and machine learning models are 138.059%, 5.00%, and 99.3%, respectively. These values suggest that a 3-20-20-1 back propagation ANN outperformed both random forest and MRA models.

2. The value of the MSE of the ANN model is 0.0098379, which indicates that the prediction can be done with a minimum error.

3. The regression value of the ANN model is much closer to 1, suggesting the fact that it can predict the surface roughness values with higher accuracy.

4. It is noticed that there is a good agreement between the ANN-predicted results and the corresponding experimental values for both training as well as testing cases. The cumbersome task of conducting the experiments can be eliminated, and also it makes the evaluation of the surface roughness more economically viable.

5. In turning of GFRP, the spindle speed influenced the most followed by feed rate and depth of cut.

References

[1] D. T. Hull and W. Clyne,"An introduction to composite materials," *2nd ed., Cambridge univ. press*, (1996).

[2] T. Rajasekaran, K. Palanikumar and B. K. Vinayagam, "Turning CFRP composites with Ceramic tool for Surface Roughness Analysis," *Procedia Eng.*, Vol. 38, No. 1, pp. 2922–2929, (2012).

[3] P. M. M. S. Sarma, L. Karunamoorthy and K. Palanikumar, "Surface Roughness Parameters Evaluation in Machining GFRP Composites by PCD Tool using Digital Image Processing," *J. Reinf. Plast. Compos.*, Vol. 28, No.13, pp.1567-1585, (2009).

[4] K. Palanikumar, B. Latha, V. S. Senthilkumar and J. P. Davim, "Analysis on Drilling of Glass Fiber–Reinforced Polymer (GFRP) Composites Using Grey Relational Analysis," *Mater. Manuf. Processes.*, Vol. 27, No. 3, pp. 297-305, (2012).

[5] I. S. N. V. R. Prashanth and B. Chandra Mouli, "Critical Analysis in Milling of GFRP Composites by Various End Mill Tools," *Mater. Today. Proc.*, Vol. 5, No. 6, pp.14607-14617, (2018).

[6] A. I. Azmi, R. J. T. Lin and D. Bhattacharyya, "Experimental Study of Machinability of GFRP Composites by End Milling," *Mater. Manuf. Processes*, Vol. 27, No.10, pp. 1045-1050, (2012).

[7] I. Shivakoti, G. Kibria, P. M. Pradhan, B. B. Pradhan and A. Sharma, "ANFIS based prediction and parametric analysis during turning operation of Stainless Steel 202," *Mater. Manuf. Processes*, Vol. 34, No. 1, pp.112-121, (2019).

[8] N. Manikandan, K. Balasubramanian, D. Palanisamy, P.M. Gopal, D. Arul Kirubakaran and J. S. Bihoj, "Machinability analysis and ANFIS modelling on Advanced Machining of Hybrid Metal Matrix composite for Aerospace applications," *Mater. Manuf. Processes*, Vol. 34, No.16, pp.1866-1881, (2019).

[9] K. Balasubramanian, M. Nataraj and P. Duraisamy, "Machinability analysis and application of response surface approach on CNC turning of Lm6/SiC pcomposites," *Mater. Manuf. Processes*, Vol. 34, No. 12, pp. 1389-1400, (2019).

[10] V. Varghese, M. K. Ramesh and D. Chakradhar, "Experimental Investigation and optimization of machining parameters for sustainable machining," *Mater. Manuf. Processes*, Vol. 33, No.16, pp.1782-1792, (2018).

[11] D.Priyadarshi and R. Kumarsharma, "Optimization for turning of Al6061-SiC-Gr Hybrid Nanocomposites using Response Surface Methodology", *Mater. Manuf. Processes*, Vol. 31, No. 10, pp. 1342-1350, (2016).

[12] V. Mukkoti, G. Sankaraiah and M. Yohan, "Effect of cryogenic treatment of Tungsten carbide tools on Cutting force and power consumption in CNC milling process,"*Mater. Manuf. Processes*, Vol. 6, No. 1, pp.149-170, (2018).

[13] K. Palanikumar, L. Karunamoorthy, R. Karthikeyan and B. Latha, "Optimization of machining parameters in turning GFRP composites using a carbide (K10) tool based on the taguchi method with fuzzy logics," *Met. Mater.*, Vol. 12, No. 6, pp. 483-491, (2006).

[14] K. Palanikumar, L. Karunamoorthy and R. Karthikeyan, "Multiple Performance Optimization of Machining Parameters on the Machining of GFRP Composites Using Carbide (K10) Tool," *Mater. Manuf. Processes,* Vol. 21, No. 8, pp. 846-852, (2006).

[15] H.Charukar and T. L. Schmitz, "A neural network approach for chatter prediction in turning,"*Procedia Manufacturing*, Vol. 34, No. 1, pp. 885-892, (2019).

[16] B. Goel, S. Singh and R. V.Sarepaka, "Optimizing single point diamond turning for mono crystalline Germanium using Grey regression Analysis," *Mater. Manuf. Processes*, Vol. 30, No. 8, pp. 1018-1025, (2015).

[17] R. Ferreria, D. Carou, C. H. Lauro and J. P. Davim, "Surface roughness investigation in the hard turning of steel using Ceramic tools," *Mater. Manuf. Processes*, Vol. 31, No. 5, pp. 648-652, (2016).

[18] P. M. M. S. Sarma, L. Karunamoorthy and K. Palanikumar,, "Modeling and Analysis of Cutting Force in Turning of GFRP Composites by CBN Tools," *J. Reinf. Plast. Compos.*, Vol. 27, No. 7, pp. 711-723, (2008).

[19] P. Mistry, D. Neagu, P. R. Trundle and J. D. Vessey, "Using random forest and decision tree models for a new vehicle prediction approach in computational toxicology," *Soft. Computing.*, Vol. 20, No. 8, pp. 2967–2979, (2016).

[20] P. Zhou, Z. Li, S. Snowling, B. W. Baetz, D. Na and G. Boyd, "A random forest model for inflow prediction at wastewater treatment plants," *Stoch. Environ. Res. Risk. Assess.*, Vol. 33, No. 10, pp. 1781–1792, (2019).

[21] J. Zhang, M. Li, Y. Feng and C. Yang, "Robotic grasp detection based on image processing and random forest," *Multimed. Tools. Appl.*, Vol. 79, No. 3, pp. 2427–2446, (2020).

[22] S. Kwak, J. Kim, H. Ding, X. Xu, R. Chen, J. Guo and H. Fu"Machine learning prediction of the mechanical properties of γ-TiAl alloys produced using random forest regression model," *J. Mater. Res. Technol.*, Vol. 18, No.1, pp. 520-530, (2022).

[23] J. Wang, Z. Song, L. Chen, T. Xu, L. Deng and Z. Qi, "Prediction of CO_2 solubility in deep eutectic solvents using random forest model based on COSMO-RS-derived descriptors," *Green. Chem. Eng.*, Vol. 2, No. 4, pp. 431-440, (2021).

[24] Y. Liu, S. Chen, J. Ye, Y. Xian, X. Wang, J. Xuan, N. Tan, Q. Li, J. Chen and Z. Ni," Random forest for prediction of contrast-induced nephropathy following coronary angiography," *Int J Cardiovasc Imaging*, Vol. 36, No.6, pp. 983–991, (2020).

[25] F. J. Pontes, A. P. de Paiva, P. P.Balestrassi, J. R. Ferreira andM. B. da Silva, "Optimization of Radial Basis Function neural network employed for prediction of surface roughness in hard turning process using Taguchi's orthogonal arrays," *Expert Systems with Applications*, Vol. 39, No. 9, pp. 7776-7787, (2012).

How to cite this paper: